Gelsolin Associates with the N Terminus of Syntaxin 4 to Regulate Insulin Granule Exocytosis

Michael A. Kalwat, Dean A. Wiseman, Wei Luo, Zhanxiang Wang, and Debbie C. Thurmond

Departments of Biochemistry and Molecular Biology (M.A.K., D.C.T.) and Pediatrics (D.A.W., Z.W., D.C.T.), Indiana University School of Medicine, Indianapolis, Indiana 46202; and GenScript Corp. (W.L.), Piscataway, New Jersey 08854

The plasma membrane soluble N-ethylmaleimide-sensitive factor attachment receptor (SNARE) protein syntaxin (Syn)4 is required for biphasic insulin secretion, although how it regulates each phase remains unclear. In a screen to identify new Syn4-interacting factors, the calcium-activated F-actin-severing protein gelsolin was revealed. Gelsolin has been previously implicated as a positive effector of insulin secretion, although a molecular mechanism to underlie this function is lacking. Toward this, our *in vitro* binding studies showed the Syn4-gelsolin interaction to be direct and mediated by the N-terminal Ha domain (amino acid residues 39–70) of Syn4. Syn4-gelsolin complexes formed under basal conditions and dissociated upon acute glucose or KCl stimulation; nifedipine blocked dissociation. The dissociating action of secretagogues could be mimicked by expression of the N-terminal Ha domain of Syn4 fused to green fluorescent protein (GFP) (GFP-39–70). Furthermore, GFP-39–70 expression in isolated mouse islet and clonal MIN6 β-cells initiated insulin release in the absence of appropriate stimuli. Consistent with this, the inhibitory GFP-39–70 peptide also initiated Syn4 activation in the absence of stimuli. Moreover, although MIN6 β-cells expressing the GFP-39–70 peptide maintained normal calcium influx in response to KCl, KCl-stimulated insulin secretion and the triggering pathway of insulin secretion were significantly impaired. Taken together, these data support a mechanistic model for gelsolin's role in insulin exocytosis: gelsolin clamps unsolicited soluble N-ethylmaleimide-sensitive factor attachment receptor (SNARE)-regulated exocytosis through direct association with Syn4 in the absence of appropriate stimuli, which is relieved upon stimulus-induced calcium influx to activate gelsolin and induce its dissociation from Syn4 to facilitate insulin exocytosis. **(*Molecular Endocrinology* 26: 128–141, 2012)**

NURSA Molecule Pages[†]: Coregulators: GSN.

In response to a sharp increase in glucose concentration, such as that induced by intake of a meal, pancreatic islet β-cells secrete insulin, doing so in a highly regulated and biphasic manner (1). The first phase is rapid and robust, occurring within 10 min of stimulation, and thought to be accounted for by a readily releasable pool of granules already present at the plasma membrane (PM). The second phase follows at a sustained, lower rate of secretion that can last for hours (2) and is elicited only in response to fuel-type secretagogues, such as glucose. In order for insulin to be secreted, insulin granules must fuse with the PM in a stimulus-dependent and highly regulated manner; this process is carried out by soluble N-ethylmaleimide-sensitive factor attachment receptor (SNARE) proteins (3–6). Two known functional target membrane-SNARE (t-SNARE) isoforms from the syntaxin (Syn) protein family, Syn1A and Syn4, facilitate selective insulin granule fusion in β-cells via functioning as docking sites at the PM; Syn1A is

ISSN Print 0888-8809 ISSN Online 1944-9917
Printed in U.S.A.

doi: 10.1210/me.2011-1112 Received May 30, 2011. Accepted October 24, 2011.
First Published Online November 22, 2011

[†] Annotations provided by Nuclear Receptor Signaling Atlas (NURSA) Bioinformatics Resource. Molecule Pages can be accessed on the NURSA website at www.nursa.org.

Abbreviations: GFP, Green fluorescent protein; GFP-39–70-Ad, adenovirus encoding GFP-39–70; GFP-Scr, GFP fused to scrambled peptide; GST, glutathione *S*-transferase; K_{ATP}, ATP-sensitive potassium channel; LAT, latrunculin B; MKRBB, modified Krebs-Ringer bicarbonate buffer; NP-40, Nonidet P-40; PAK1, p21-activated kinase-1; PM, plasma membrane; PVDF, polyvinylidene fluoride; SNARE, soluble N-ethylmaleimide-sensitive factor attachment receptor; Syn, syntaxin; TM, transmembrane domain; t-SNARE, target membrane-SNARE; VAMP2, vesicle-associated membrane protein-2.

required only for first phase secretion, whereas Syn4 is important for both first and second phases (7, 8). Both Syn isoforms pair with a second t-SNARE, SNAP-25 (synaptosomal-associated protein-25), under both unstimulated/basal and stimulated conditions (9, 10). Insulin granules are equipped with the vesicle-SNARE protein vesicule-associated membrane protein-2 (VAMP2)/synaptobrevin (11) and, upon arrival at the PM, form heterotrimeric SNARE core complexes by docking with t-SNARE to facilitate membrane fusion (reviewed in Refs. 12, 13). Importantly, insulin release must be clamped under basal conditions, to provide the steep gradient necessary for a regulated stimulus response to appropriate secretagogues. Defects in clamping unsolicited insulin exocytosis are associated with elevated basal insulin levels and are disruptive to maintenance of glucose homeostasis *in vivo* (14).

To sustain insulin release, mature insulin granules in intracellular storage pools must be mobilized toward the PM. This process appears to coincide with glucose-induced remodeling of the actin cytoskeleton (9, 15, 16). Filamentous actin (F-actin) functions as a barrier to restrain insulin granule accumulation at the PM (17, 18), such that its depolymerization results in more morphologically docked granules and may confer release competence (10, 19). Evidence of positive effects of the cytoskeleton in stimulus-induced insulin secretion exists as well (20–23). In fact, insulin granules are known to interact with F-actin filaments and require microtubule tracks, upon which to traffic to the F-actin network toward the PM (24–26). Beyond impact upon trafficking, disruption of F-actin remodeling with agents that induce either F-actin disassembly or polymerization reveals that both actions jointly impact stimulated exocytosis outcomes (27). F-actin reorganization is important for stimulated exocytosis in many cell types other than β-cells, including neuroendocrine cells, adrenal chromaffin cells, platelets, and endothelial cells (28–30). In addition to controlling stimulated exocytosis, the actin cytoskeleton affects control of basal exocytosis through focal adhesion kinase, EphA-Ephrin-A signaling, and cell contact (23, 31, 32). However, molecular mechanisms to describe how the cytoskeleton might participate in clamping of exocytotic machinery to ensure low levels of insulin secretion in the absence of stimuli remain unresolved.

Multiple SNARE proteins are linked with the F-actin cytoskeleton (10, 28, 33), although only Syn4 can directly interact with F-actin *in vitro*. Granule docking at Syn4 sites may be an important limiting factor in insulin exocytosis, given that increasing the number of Syn4 docking sites *in vivo* augments biphasic insulin secretion while maintaining normal low basal levels (7). Syn4 binds to F-actin via a spectrin-like region within the first two coiled-coil domains of the N terminus of Syn4 (10). Use of this region as a competitive peptide inhibitor reduces endogenous F-actin-Syn4 complex formation, concomitant with enhanced glucose-stimulated insulin secretion from MIN6 β-cells. Although these data argue that F-actin anchors at Syn4 sites at the PM, the potential roles of multiple actin binding proteins that are implicated in, or shown to be necessary for, proper glucose-stimulated insulin secretion have yet to be tested for integration into this particular mechanism (20, 34–36). One particular protein of interest is gelsolin, an F-actin-severing/capping protein that plays a positive role in insulin secretion and has been proposed to be important for glucose-induced F-actin remodeling, which occurs in β-cells through an undefined mechanism (36, 37).

In this study, we provide the first evidence for formation of a novel and direct interaction between Syn4 and gelsolin, mediated via the N-terminal Ha domain of Syn4. In β-cells, this complex is dissociated in response to acute glucose or KCl stimulation. Introduction of an Ha-domain peptide (amino acid residues 39–70) into MIN6 β-cells mimicked the action of these secretagogues by inducing dissociation of endogenous Syn4-gelsolin complexes. Functionally, these binding alterations were accompanied by elevated basal insulin release in mouse islet and MIN6 β-cells, coordinate with inappropriate activation of Syn4. The peptide-induced dissociation of Syn4-gelsolin complexes in MIN6 β-cells also attenuated acute glucose- and KCl-stimulated insulin exocytosis, coinciding with attenuation of the ATP-sensitive potassium channel (K_{ATP})-channel-dependent triggering pathway in the diazoxide paradigm. These data support a new model for a clamping mechanism underlying regulated SNARE protein-mediated exocytosis. Given that 1) gelsolin and Syn4 are ubiquitously expressed proteins, 2) F-actin remodeling occurs in non-β-cell types, and 3) the effects upon insulin exocytosis are not secretagogue-specific, we propose that this mechanism may be applicable to regulated exocytosis events on a broader cell biological basis.

Results

Syn4 directly interacts with gelsolin

We first identified gelsolin as a potential Syn4-binding partner in an unbiased yeast two-hybrid screen (Thurmond, D. C., and J. E. Pessin, unpublished results) and subsequently validated gelsolin protein to bind directly to recombinant soluble [lacking the C-terminal transmembrane domain (TM)] glutathione *S*-transferase (GST)-Syn4 *in vitro* (Fig. 1A). Because both Syn4 and gelsolin are required for glucose-stimulated insulin exocytosis (7,

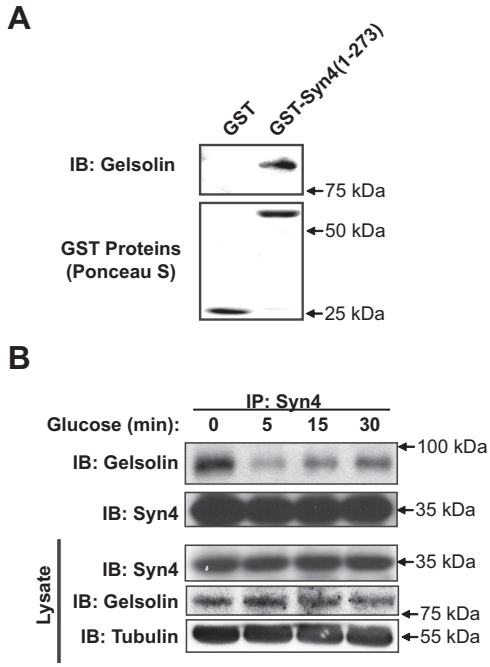

FIG. 1. Syn4 and gelsolin directly interact and form complexes in MIN6 β-cells that are sensitive to glucose stimulation. A, Recombinant gelsolin was combined with either GST or GST-Syn4 (1–273) linked to sepharose beads for a 2-h incubation at 4 C. Beads were pelleted and extensively washed, with eluates subjected to 10% SDS-PAGE for immunoblot detection (IB) of gelsolin. Ponceau staining served as control for GST protein loading. Data are representative of at least three independent experiments using two different batches of protein. B, MIN6 cells were preincubated in MKRBB for 2 h and stimulated with 20 mM glucose for 5, 15, or 30 min. Cleared detergent cell lysates were prepared and used in Syn4 immunoprecipitation (IP) reactions. Immunoprecipitates were resolved on 10% SDS-PAGE, and proteins were transferred to PVDF for immunoblot detection of Syn4 and gelsolin. Protein abundances in starting input lysates (100 μg) were confirmed on a separate gel. Data are representative of at least three independent coimmunoprecipitation studies.

36), the presence of full-length endogenous Syn4-gelsolin complexes was subsequently investigated and revealed to exist in MIN6 β-cell lysates (Fig. 1B). Notably, these complexes were found to rapidly and transiently dissociate in response to acute 5-min glucose stimulation. After a 30-min glucose stimulation, Syn4-gelsolin complex abundance resumed to approximately 50% that detected under basal conditions. Changes in complex formation were independent of changes in Syn4 or gelsolin protein abundances in cell lysates.

Given the novelty of this interaction, we next sought to identify the minimal region of Syn4 required to confer direct binding to gelsolin. Syn4 truncations fused C terminally to GST were analyzed using *in vitro* binding studies with recombinant gelsolin. As depicted in the schematic representation of Fig. 2A, Syn4 protein is composed of three N-terminal α-helical domains, which, based upon comparison with the x-ray crystal structure of family member Syn1A, pack together to comprise a coiled-coil bundle and are linked to the C-terminal α-helical SNARE domain known to be operational in binding SNARE proteins (38). Elimination of all but the N-terminal most Ha (residues 1–70) domain failed to ablate binding to gelsolin, including the Hb (residues 71–112) region previously shown to be required to confer Syn4 binding to F-actin (Fig. 2B) (10). To evaluate this binding event in a mammalian cell expression system, CHO-K1 cells were electroporated to express Flag-tagged gelsolin with truncated green fluorescent protein (GFP)-Syn4 fusion proteins (GFP-39–112 and GFP-1–70), and detergent solubilized cell lysates were prepared for coimmunoprecipitation analyses. Indeed, anti-Flag (gelsolin) immunoprecipitation coprecipitated with both truncated forms of Syn4 (Fig. 2C). After this, the far N-terminal residues 1–38 were removed to isolate the Ha domain, GFP-39–70, which was sufficient to confer binding to Flag-tagged gelsolin (Fig. 2D). Despite efforts to test for necessity of the Ha domain, deletion of the Ha from either GST- or GFP-fusion protein rendered proteins too unstable to study. Regardless, the ability of this Ha domain to confer binding to gelsolin distinguishes its interaction with Syn4 from that of F-actin, because Ha alone failed to confer Syn4 binding to F-actin (10). Importantly, this is the first demonstration of the Ha domain conferring stable binding with any of the known Syn4 binding partners.

Competitive inhibition of endogenous Syn4-gelsolin complexes

Because there are reported effects of apoptosis and compensatory cytoskeletal effects associated with gelsolin knockdown/depletion approaches (39, 40), we opted to use the Ha-domain peptide (GFP-39–70) as a competitive inhibitor in effort to selectively target the Syn4-gelsolin complex to evaluate its function in insulin exocytosis. In addition to the unusual ability of the Syn4 Ha domain to confer binding to gelsolin, as opposed to how Syn4 binds other partners, the Ha domain (residues 39–70) carries the least identity of all its helical domains (<35%) to Syn1A. Using lysates prepared from MIN6 β-cells expressing the GFP-39–70 protein, anti-Syn4 immunoprecipitation reactions resulted in attenuated coprecipitation of gelsolin under basal (unstimulated) conditions, compared with reactions from control GFP; a scrambled peptide fused to GFP (GFP-Scr), designed to retain helical structure (http://npsa-pbil.ibcp.fr), was without effect (Fig. 3A). Having established specificity of the GFP-39–70 peptide upon Syn4-gelsolin complexes, we next evaluated effects after an acute 5-min glucose stimulation. GFP-expressing cells showed reduced interaction of endogenous Syn4-gelsolin complexes in GFP-expressing cells, similar to that of complexes shown in Fig. 1B. How-

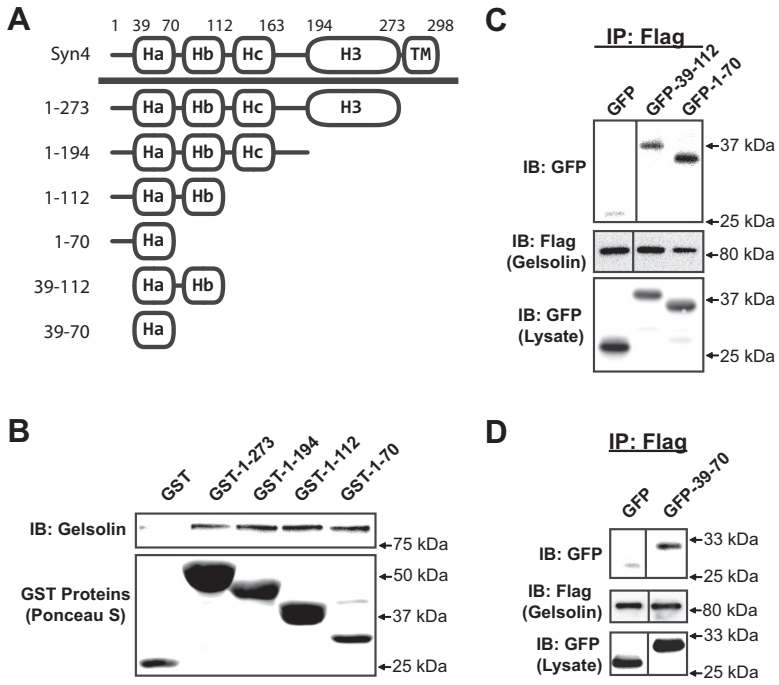

FIG. 2. Residues 39–70 of Syn4 are sufficient to confer Syn4-gelsolin binding. A, Depiction of the multiple helical domains of the Syn4 protein. The N-terminal helical domains are denoted as Ha, Hb, and Hc; the C-terminal H3 helix is the SNARE domain, followed by the TM. B, *In vitro* binding reactions containing recombinant gelsolin protein plus either GST or GST-Syn4 truncation proteins linked to beads were performed as described in Fig. 1, and proteins resolved by 10% SDS-PAGE for immunoblotting (IB). Ponceau S staining shows the presence of the GST proteins in each reaction. Data are representative of two independent experiments. CHO-K1 cells were coelectroporated with pEGFP, pEGFP-Syn4(39–112) or pEGFP-Syn4 (1–70) DNA (C), or pEGFP-Syn4(39–70) DNA along with pIRES-gelsolin-Flag DNA (D), and 48 h later, detergent lysates were prepared for immunoprecipitation (IP) with anti-Flag antibody. Immunoprecipitates were subjected to 10% SDS-PAGE for immunoblot detection of GFP and Flag (gelsolin). Input lysates (50 μg) demonstrate expression and migration of each protein. *Vertical lines* denote splicing of lanes from within the same gel. Data are representative of three independent immunoprecipitation experiments.

ever, glucose stimulation of GFP-39–70-expressing cells failed to further dissociate the endogenous complex (Fig. 3Bi). As we have previously shown that F-actin, but not G-actin, interacts with Syn4 in β-cells in a glucose-sensitive manner, and can directly interact with Syn4 *in vitro* (10), we questioned whether gelsolin was coupled to this interaction. Coordinate with this, F-actin association with Syn4 in the presence of the GFP-39–70 peptide was diminished in unstimulated cell lysates, relative to GFP alone (Fig. 3Bii). Moreover, pharmacologically induced actin depolymerization using latrunculin B (LAT) caused dissociation of both actin and gelsolin from Syn4 (Fig. 3C).

Because gelsolin knockdown in MIN6B1 cells exerted global effects upon F-actin remodeling, we investigated this as a potential explanation for the GFP-39–70-induced alterations to Syn4 binding. We first determined that selective attenuation of Syn4-gelsolin binding under basal conditions was unattributable to differential GFP-39–70 subcellular localization, because its principally cytosolic localization was similar to that of GFP, as visualized by confocal microscopy (Fig. 4, panels 1–4). However, unstimulated GFP-39–70-expressing cells contained contiguous cortical F-actin (red, rhodamine-phalloidin staining) similar to that of neighboring untransfected cells and of GFP control cells (Fig. 4, panels 5 and 6, and 9 and 10). Moreover, GFP and GFP-39–70-expressing cells all showed the expected acute glucose-induced actin remodeling, as determined by disruption of the contiguous cortical F-actin rim encircling each cell (Fig. 4, panels 7 and 8, and 11 and 12). These data indicated that the GFP-39–70 peptide sufficed as a competitive inhibitor of endogenous Syn4-gelsolin complexes present in unstimulated MIN6 β-cells and did so without inducing global changes in cortical F-actin structure.

Syn4-gelsolin complexes are required to clamp unsolicited insulin exocytosis events

The competitive peptide was subsequently used to determine the functional ramifications of disrupting Syn4-gelsolin complexes upon insulin secretion from isolated islets and MIN6 cells. To ensure thorough and efficient expression of the peptide across cell populations for these studies, an adenovirus encoding GFP-39–70 (GFP-39–70-Ad) was generated and validated to exert dissociating actions upon endogenous Syn4-gelsolin complexes akin to that of the plasmid-based delivery system (Supplemental Fig. 1A, published on The Endocrine Society's Journals Online web site at http://mend.endojournals.org). Subsequently, islets isolated from wild-type C57BL/6J mice were transduced with GFP-39–70 or GFP adenoviruses and protein expression confirmed (Fig. 5A), albeit GFP-39–70 expression was consistently lower than that of GFP. Islet perifusion experiments were initiated to examine effects of GFP-39–70 expression upon basal and phasic insulin release. GFP-39–70-expressing islets released approximately 4-fold more insulin under basal (2.8 mM glucose) conditions (Fig. 5B), and first phase secretion appeared to be slightly impaired in GFP-39–70-expressing islets (GFP-39–70 peaked 3-fold above basal, GFP peaked 10-fold above basal). However, defective basal secretion impeded reliability of area under the curve analysis to quantify phasic differences. We next employed a short-term static

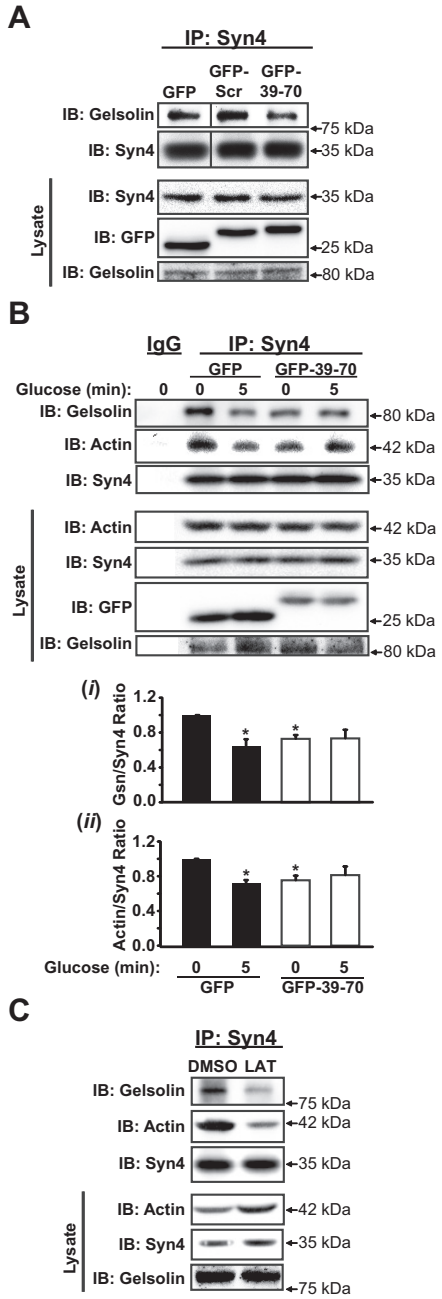

FIG. 3. GFP-39–70 disrupts endogenous Syn4-gelsolin complexes. A, MIN6 cells transfected to express GFP, GFP-39–70, or GFP-Scr (scrambled peptide) were preincubated in MKRBB for 2 h and resultant lysates used for anti-Syn4 immunoprecipitation (IP). Coprecipitated proteins were resolved on 10% SDS-PAGE for immunoblot detection (IB). Data represent at least three independent coimmunoprecipitation experiments. B, MIN6 cells transfected to express either GFP or GFP-39–70 proteins were preincubated and stimulated with 20 mM glucose for 5 min; lysates were used in IP reactions as detailed in A above. Band intensities of actin and gelsolin association with Syn4 were quantitated and expressed as the ratio of gelsolin (*Gsn*) (i) and actin (ii) to Syn4 (normalized, basal ratio = 1 for each experiment). *Bars* represent the mean ± SE of the three independent experiments (*, $P < 0.05$, *vs.* unstimulated GFP). C, MIN6 cells were treated with vehicle [dimethylsulfoxide (DMSO)] or 10 μM LAT for 2 h in MKRBB and resultant cell lysates used for IP as described in A and B above in three independent experiments. Protein abundances in starting input lysates (100 μg) were confirmed on a separate gel. *Vertical lines* denote splicing of lanes from within the same gel.

incubation approach as a means to quantify acute/first phase secretion using glucose or KCl secretagogues. Again, basal elevation in GFP-39–70-expressing cells was fully recapitulated in the static culture system, yet short term-stimulated secretions were highly erratic and thwarted efforts to discern significant first phase differences (Fig. 5C). However, this rise in basal secretion in GFP-39–70 islets nearly abolished the overall stimulatory responses compared with those of GFP-expressing islets (stimulation index = glucose-stimulated/basal secretion) (Fig. 5D). Differences in secretion were not due to alterations in insulin content (Fig. 5E). No significant differences in long-term glucose-stimulated insulin secretion (1 h) or associated insulin content were noted between GFP and GFP-39–70-expressing islets (Supplemental Fig. 1, B and C). These data suggested that dissociation of endogenous Syn4-gelsolin complexes under basal conditions permitted or otherwise prompted inappropriate insulin release.

Loss of clamping of basal insulin release could result from a direct effect upon Syn4 activation, or possibly an indirect effect of aberrant Cdc42 signaling, as has been found to occur in other cases of dysregulated basal insulin secretion (41, 42). To test for alterations in Syn4 activation, lysates prepared from MIN6 β-cells transduced to express GFP or GFP-39–70 protein were combined with recombinant GST-VAMP2 (soluble, TM domain deleted) protein, linked to sepharose beads, as a means to selectively precipitate open conformation Syn4 as described previously (10, 41). It is expected that opening increases accessibility of Syn4 to enhance granule docking to promote granule fusion and insulin release. Although GFP-expressing cells exhibited a low level of basal activation and responded to acute glucose stimulation (5 min) with the traditional approximately 2-fold increase in Syn4 activation, GFP-39–70-expressing cells showed significantly elevated basal Syn4 activation, with no further responsiveness to glucose (Fig. 6A). These differences were not a consequence of differential Syn4 protein expression, or between GFP and GFP-39–70 in the starting lysates (Fig. 6B). Further implicating Syn4 activation as a mechanism to explain elevated basal secretion, Cdc42 signaling was unaffected by the GFP-39–70 peptide, as gauged by normal activation (phosphorylation) levels of the immediate downstream Cdc42 effector protein [p21-activated kinase-1 (PAK1)] under basal conditions (Fig. 6C).

Syn4-gelsolin complexes and the K_{ATP} channel-dependent/triggering pathway in MIN6 β-cells

Islets are composed of multiple cell types. To ascertain whether erratic short-term insulin secretion outcomes from islet studies were due to possible effects of noninsulin-secret-

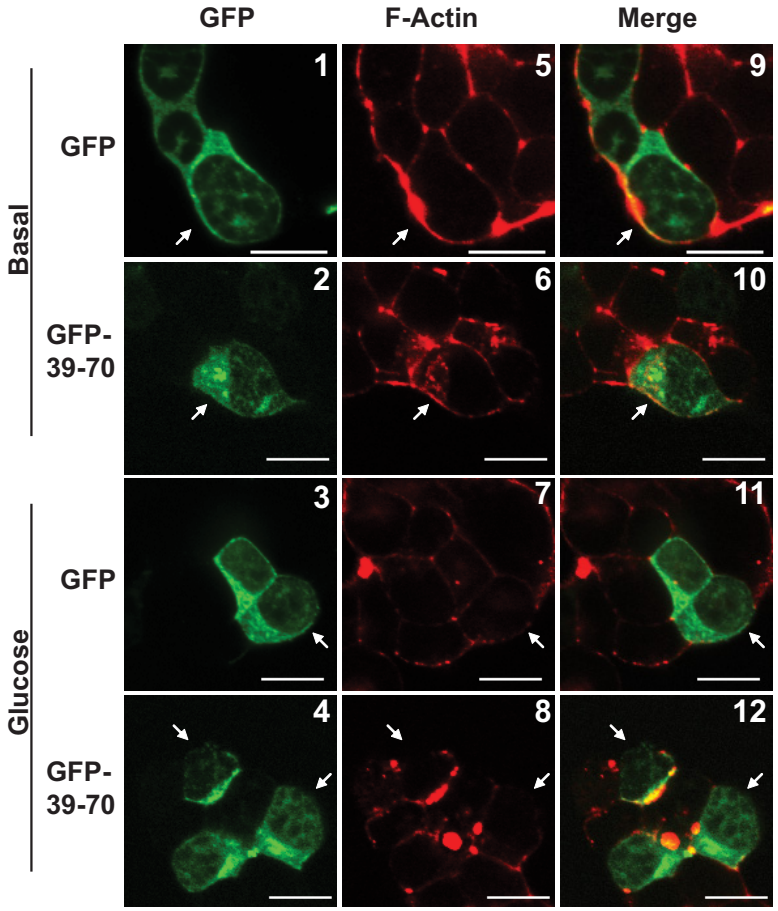

FIG. 4. GFP-39–70 does not disrupt normal glucose-induced actin remodeling. MIN6 cells were plated on glass coverslips and transfected to express GFP or GFP-39–70 proteins (*green*) were preincubated in MKRBB for 2 h and left unstimulated (*top* panels 1 and 2, 5 and 6, and 9 and 10) or stimulated with 20 mM glucose for 5 min (*bottom* panels 3 and 4, 7 and 8, and 11 and 12). Cells were fixed, permeabilized, and cortical F-actin staining detected by rhodamine-phalloidin staining (*red*). Cells in clusters containing both nontransfected and GFP-transfected cells were imaged at the midplane of the cluster by single channel scanning confocal microscopy to determine subcellular distribution of the GFP proteins (panels 1–4) and F-actin remodeling (panels 5–8). Merged GFP and F-actin images are shown in panels 9–12 to permit comparisons between nontransfected and transfected cells. *Scale bar*, 10 μm. Data shown are representative of three independent sets of experiments.

ing cell types within islets, secretion studies were performed in the clonal MIN6 β-cell system. Mouse clonal MIN6 cells are considered to have similar insulin content and glucose-stimulatory response similar to that of normal islets, where normal responses occur at 16–20 mM glucose (43). As observed in mouse islets, expression of the GFP-39–70 but not the GFP-Scr peptide in MIN6 cells induced elevation of basal secretion in the absence of secretagogue (Fig. 7A and Supplemental Fig. 2), although to a lesser extent than observed in whole islets. Similar to islets, prolonged glucose stimulation failed to unveil significant differences in insulin release between GFP and GFP-39–70-expressing cells (data not shown). By contrast, acute stimulation (10 min) with either glucose or KCl in GFP-39–70-expressing cells elicited small but significant approximately 20% attenuations of acute (10 min) stimulus-induced secretion (Supplemental Fig. 3): 20 mM glucose (205 ± 22 and 169 ± 20 ng/mg protein for GFP *vs.* GFP-39–70, respectively) and with 35 mM KCl (499 ± 48 and 410 ± 24 ng/mg protein for GFP *vs.* GFP-39–70, respectively). The combined impairments in basal and secretagogue-stimulated secretion culminated in significant losses in stimulation index (Fig. 7B) and were not due to GFP-39–70-induced β-cell apoptosis, as evaluated by caspase-3 cleavage (Fig. 7C).

Another method used to assess the phases of glucose stimulation is by the diazoxide paradigm. This pharmacological paradigm is based upon the premise that the first phase release is due to K_{ATP}-dependent triggering, whereas the second phase is regulated by K_{ATP} channel-independent amplifying effects (44–47). By subjecting MIN6 β-cells to depolarizing KCl concentrations in the presence of the K_{ATP} channel opener diazoxide, low glucose simulates triggering, and high glucose simulates amplification (34). Using this paradigm, GFP-39–70-expressing cells showed approximately 30% decrease in the KCl-stimulated triggering of insulin secretion compared with GFP-expressing controls (Fig. 8A). Diazoxide action was verified by abolishment of secretion from cells treated with diazoxide alone or in combination with glucose in the absence of depolarizing KCl concentrations (data not shown). The GFP-expressing cells exhibited the amplifying response, with approximately 3-fold more insulin release upon stimulation with glucose, validating responsiveness of the cells (34, 48). However, the stimulation index of the amplification effect between GFP- and GFP-39–70-expressing cells was similar (Fig. 8A, *inset graph*). This suggested that artificial disruption of the Syn4-gelsolin complex by the GFP-39–70 peptide may have compromised triggering. However, efforts to use this paradigm in adenovirally transduced islets failed, because a combination of these islets and diazoxide treatment dramatically reduced insulin content (data not shown).

We next determined whether triggering steps impacted the Syn4-gelsolin complex dissociation. The triggering

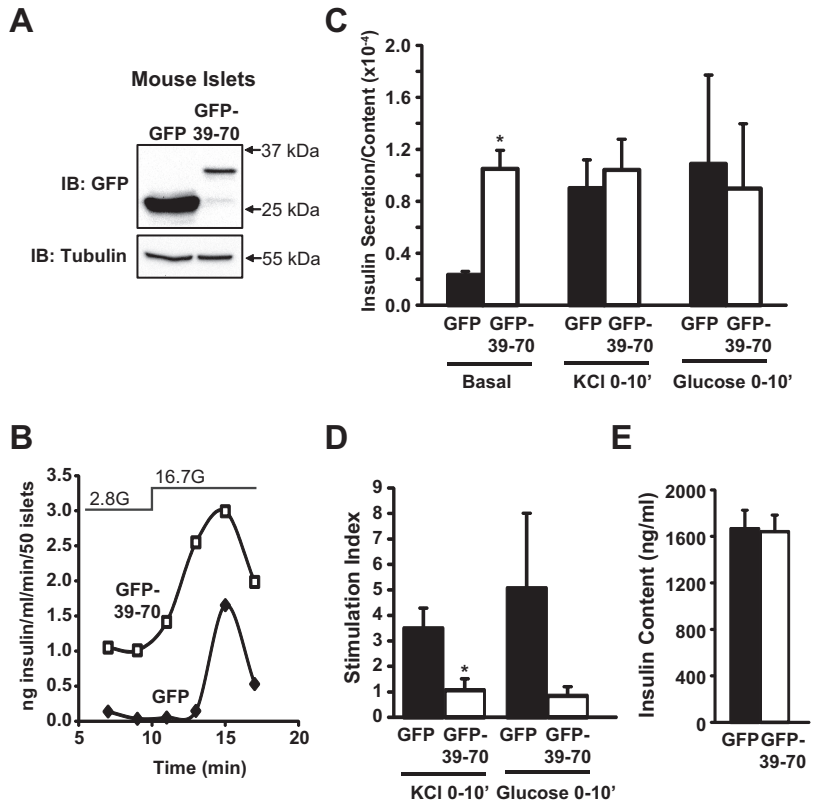

FIG. 5. Disruption of Syn4-gelsolin complexes elevates basal insulin secretion from isolated mouse islets. Freshly isolated mouse islets were immediately transduced with GFP or GFP-39–70 adenovirus, and after a 48-h incubation, GFP-positive islets were handpicked under a fluorescence microscope for immunoblot analysis (A), for perifusion analysis (B), and for static culture studies (C). Perifusion entailed use of 50 GFP positive islets per column with GFP and GFP-39–70-expressing islet columns run in parallel; islets were perifused with low glucose (2.8 mM) followed by high glucose (16.7 mM) to capture first phase release. Static secretion reactions contained 10 GFP positive islets/tube and were incubated in low glucose (2.8 mM) KRBH for 2 h and buffer collected for quantitation of basal insulin secretion. Buffers containing stimulatory levels of glucose (16.7 mM) or KCl (35 mM) were added to the islets for 10 min, followed by collection for insulin quantitation. Insulin content in the remaining islets was also determined and used to normalize insulin secretion data; *, $P < 0.001$ *vs.* GFP. D, Stimulation index was calculated using the values from C (stimulated insulin release/basal insulin release). E, Insulin content was similar between transduced islet groups. Data represent the mean ± SE of three independent islet isolation experiments; *, $P < 0.05$ *vs.* GFP. IB, Immunoblotting.

pathway is defined as that involving closure of K_{ATP} channels, membrane depolarization, opening of voltage-dependent calcium channels, calcium influx and rise in the cytoplasmic-free calcium concentration ($[Ca^{2+}]_c$), and activation of the exocytotic machinery (49). Testing these steps, acute KCl stimulation dissociated Syn4-gelsolin complexes (Fig. 8B). Consistent with this, treatment with nifedipine, which blocks calcium influx through the β-cell's voltage-dependent calcium channels, blocked glucose-induced dissociation of endogenous Syn4-gelsolin complexes (Fig. 8C). However, fura 2 calcium imaging experiments revealed no decrease in KCl-stimulated increases in $[Ca^{2+}]_c$ in GFP-39–70-Ad-expressing cells *vs.* GFP cells (Fig. 8D), suggesting that the GFP-39–70 peptide does not disrupt Syn4-gelsolin complexes and acute insulin secretion via disrupting calcium influx/elevation of $[Ca^{2+}]_c$ *per se*. Taken together with the abnormal activation of SNARE machinery (Syn4) induced by the GFP-39–70 peptide data of Fig. 6, these data support the conclusion that a stimulatory defect induced by the GFP-39–70 peptide was downstream of calcium influx/elevated $[Ca^{2+}]_c$, perhaps at steps of gelsolin activation and/or SNARE-mediated granule docking/fusion. Indeed, the calcium sensitivity of gelsolin activation is approximately 300-1000 nM, consistent with that of insulin exocytosis (50, 51).

Discussion

In this report, we demonstrate the existence of a novel interaction between the SNARE protein Syn4 and the F-actin-severing/capping protein gelsolin and that this interaction was susceptible to disruption upon glucose and KCl stimulation in β-cells. Introduction of a competitive inhibitory peptide, GFP-39–70, into pancreatic β-cells disrupted endogenous Syn4-gelsolin complexes under basal conditions, mimicking the action of secretagogue stimulation, providing strong evidence for a crucial functional role for this complex in clamping unsolicited basal insulin secretion. Mechanistically, disruption of Syn4-gelsolin complexes spurred inappropriate activation of Syn4 under basal conditions, consistent with the concept of gelsolin binding to Syn4 to mitigate unsolicited Syn4-mediated granule docking/fusion events. In addition to a role in the clamping mechanism, data gained from MIN6 cells suggest that Syn4-gelsolin complexes may also participate in the calcium- and K_{ATP} channel-dependent/triggering mechanism of insulin release, although further studies will be required to substantiate this possibility in primary cells. Such a dual action of Syn4-gelsolin complexes would be consistent with very recent work showing that actin filaments both prevent and augment the exocytosis of a single regulated secretory granule (52).

Gelsolin is a known calcium-activated F-actin severing/capping protein consisting of six homologous domains, each of which contains calcium binding sites that

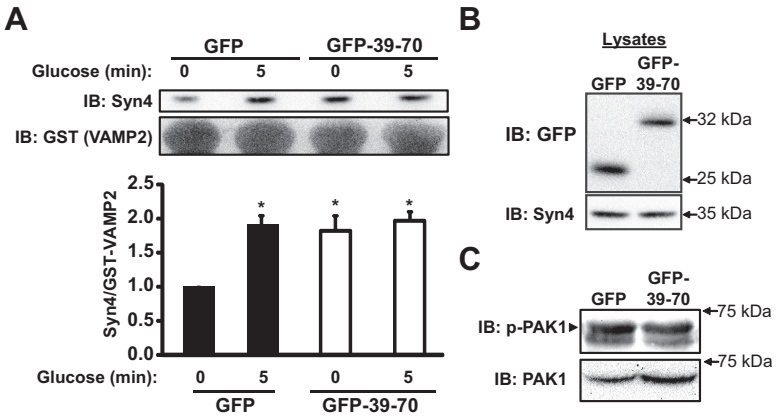

FIG. 6. Disruption of Syn4-gelsolin complexes triggers Syn4 activation in the absence of secretagogue stimulation. A, MIN6 cells transduced to express either GFP or GFP-39–70 proteins were preincubated in MKRBB for 2 h and left unstimulated or stimulated with 20 mM glucose for 5 min to generate cleared detergent cell lysates for use in GST-VAMP2 interaction assays. Lysate protein (2–3 mg) was combined with GST-VAMP2 (soluble, TM domain deleted) bound to glutathione sepharose beads, incubated for 2 h and precipitated proteins resolved on 10% SDS-PAGE for immunoblot detection (IB) of Syn4 and GST. Band intensities of Syn4 association with GST-VAMP2 were quantitated and the ratio of Syn4 to GST-VAMP2 determined (normalized to unstimulated GFP-Ad = 1 in each experiment); *, $P < 0.05$ *vs.* unstimulated GFP. B, Immunoblot to demonstrate the relative expression of GFP and GFP-39–70 proteins in the starting lysates used in GST-VAMP2 interaction assays. C, Basal Pak1 phosphorylation was evaluated by immunoblotting lysates prepared from transduced and unstimulated MIN6 cells. The marker indicates the *upper* phospho-Pak1 band; *lower* band is nonspecific. Blots were subsequently stripped and reprobed for total Pak1 protein. Images are representative of three independent sets of transduced cell lysates.

contribute to calcium-induced alterations to gelsolin's conformation and activity (50, 53–55). Because gelsolin is activated by calcium at levels observed in KCl- and glucose-stimulated β-cells (50, 51), it could be speculated that gelsolin participates within calcium microdomains for F-actin clearance at active sites of exocytosis. If so, one explanation for the effect of the GFP-39–70 peptide is that it displaced Syn4 from a calcium microdomain. However, Syn4 remains at the PM in cells treated with LAT, and moreover, that Syn4 is activated (10) and presumed to be functional given the potentiating effect of LAT upon calcium-stimulated insulin release (9). Regarding gelsolin's role at calcium microdomains for actin clearance, this remains controversial: gelsolin knockdown in the MIN6B1 cell line ablated glucose-induced F-actin remodeling, but the recent analyses of islets from gelsolin knockout mice do not show effects upon F-actin remodeling (56), and now, we also show that the GFP-39–70 peptide fails to impact actin remodeling. The lack of effect of the GFP-39–70 peptide upon actin remodeling under basal conditions could be explained by the need for calcium activation of gelsolin and that its mere dissociation from Syn4 was insufficient to induce actin remodeling. Moreover, the absence of a refractory response from the cytoskeleton to the competitive peptide could suggest that gelsolin's severing activity was unaffected by the peptide. As such, the GFP-39–70 peptide would likely not induce the many and diverse defects associated with gelsolin knockout or knockdown, such as compensatory increases in Rac1 protein, reduced fibroblast motility, and neurological and immune system defects (40, 57, 58), and did not cause apoptosis as was observed in gelsolin-depleted MIN6B1 cells (39). Because the degree of change in stimulated insulin secretion was similar in cells depleted of gelsolin (36%) and those expressing the GFP-39–70 peptide (~30%), the implication is that gelsolin's mechanism of action in glucose-stimulated insulin secretion might be through its interaction with Syn4. This may be further impacted by phosphoinositide binding and regulation of gelsolin (59–61). The lack of a larger deficit in insulin secretion could be due to compensation by a closely related family member, scinderin, which shows expression only in adrenal chromaffin cells, kidney and intestinal cells (62), and pancreatic β-cells (data not shown). Scinderin and gelsolin share more than 60% sequence identity, and a scinderin-derived actin-binding peptide inhibited Ca^{2+}-dependent exocytosis without affecting the whole-cell Ca^{2+} current, by 61% in mouse pancreatic β-cells (63). Thus, the potential remains that gelsolin and scinderin work in an additive manner, perhaps via Syn4; due to scinderin's more limited expression profile, Syn4-scinderin complexes in the β-cell could present a means to selectively manipulate insulin release.

Poorly regulated/constitutive and nonsecretagogue-specific insulin release from an islet β-cell is characteristic of an aberration of the regulated exocytosis (SNARE protein) machinery; F-actin, which is shown to function both in preventing unsolicited basal exocytosis and in promoting secretagogue-induced exocytosis in endothelial cells (52), may also be defective. Syn4 activation appears to be linked to its association with F-actin, which vacillates in the presence of secretagogue (10). As such, one possible reason that the GFP-39–70 peptide disrupted both basal and stimulated secretion in the MIN6 cells is that it may have interfered with normal activation/deactivation cycling of Syn4: after fusion, SNARE complexes undergo disassembly with t-SNARE proteins deactivated and recycled for subsequent rounds of docking/fusion. Furthermore, residues within the t-SNARE and vesicle-SNARE proteins that become surface exposed upon conformational changes induced by assembly into the heterotri-

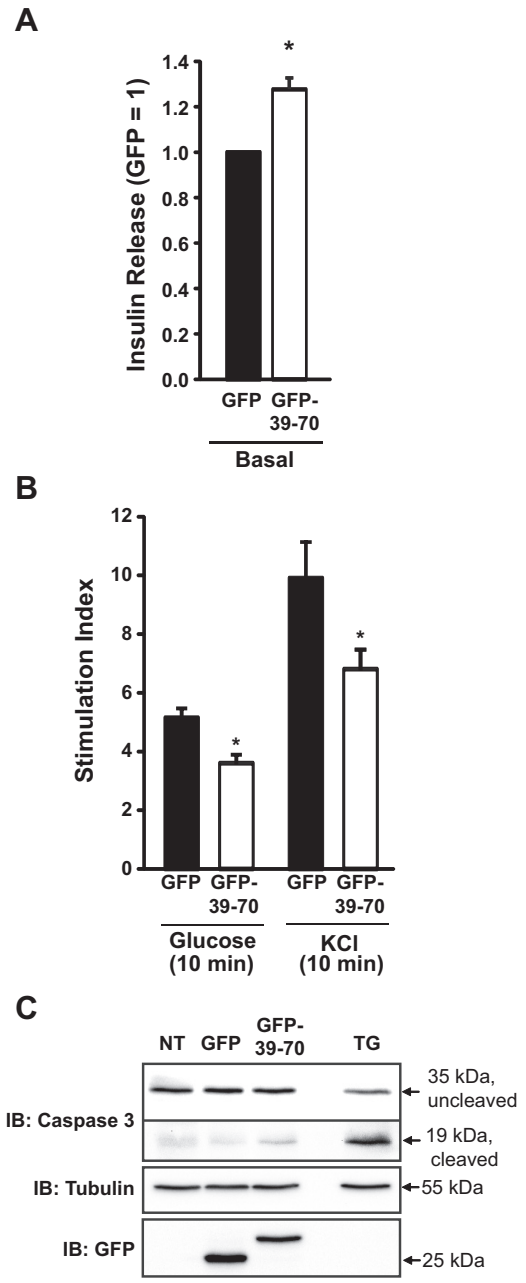

FIG. 7. Disruption of Syn4-gelsolin complexes impairs insulin secretion from MIN6 β-cells. MIN6 cells transduced to express either GFP or GFP-39–70 proteins were preincubated in MKRBB for 2 h and left unstimulated (A) or were stimulated with either 20 mM glucose or 35 mM KCl for 10 min (B) to determine the insulin secretion stimulation index (stimulated insulin release/basal insulin release). Data represent the mean ± SE of at least three independent islet batches; *, $P < 0.05$ *vs.* GFP. C, Caspase cleavage was assessed in MIN6 cells transduced to express GFP or GFP-39–70 by immunoblotting (IB) for caspase-3, which recognizes the 35-kDa inactive protein and the 19-kDa cleaved activated form. Treatment for 16 h with 0.5 μM thapsigargin (TG) to induce apoptosis served as a positive control. The GFP immunoblot shows expression of GFP and GFP-39–70 (NT, Not transduced) and tubulin immunoblot used as a loading control. Data are representative of two independent experiments.

meric SNARE core complex have been linked directly to calcium triggering of exocytosis from chromaffin cells (64). Because Syn1A can associate directly with the operative L-type voltage-dependent calcium channels in β-cells (65, 66), placing SNARE core complex formation at the site of calcium entry into the cell, future studies of Syn4 binding to channels will be required to determine whether this could also account for GFP-39–70 peptide-induced defects. Alternatively, constitutive Syn4 activation induced by the peptide could have disrupted binding and function of SNARE accessory proteins that bind calcium, such as synaptotagmin 7 and double C2 domain protein-b, both of which function in insulin secretion (67–70). Nevertheless, despite our use of multiple and diverse approaches, we were unable to reproducibly detect defects in first phase/triggering in GFP-39–70-expressing islets. One possibility is that the peptide exerted effects in non-β-cells of the islet, particularly because Syn4 and gelsolin are considered ubiquitously expressed proteins, and this generated sufficient "noise" in our systems to negate detection of the small expected changes in secretion. Deregulation of basal secretion in the islets was also far more substantial (4-fold) than in MIN6 β-cells, effectively blunting any further secretagogue-induced increase in stimulation index. Notably, however, actin filaments prevent hypersecretion as well as promote stimulated secretion (52). Given that changes in actin tethering to Syn4 occur in tandem with gelsolin, it remains possible that GFP-39–70 has impacted this process. Future studies use real-time imaging of in-cell Syn biosensors that distinguish open from closed conformations will be required to determine its cyclic activation patterns in primary islet β-cells.

The Ha domain of Syn4, in isolation, has not previously been shown to be sufficient to confer its binding to any other of Syn4's binding partners other than gelsolin. Syn4 directly interacts with both gelsolin and F-actin, and gelsolin directly binds to F-actin; however, it remains unknown whether the three form a heterotrimeric complex. The simultaneous dissociation of Syn4 from F-actin and from gelsolin in response to acute glucose stimulation in β-cells might support this concept, although efforts to reciprocally coimmunoprecipitate the complex from cell lysates, or efforts to capture the complex *in vitro*, were unsuccessful due to technical limitations with available reagents. As such, the inappropriate Syn4 activation could potentially be caused by the dissociation of F-actin that happens alongside disruption of the Syn4-gelsolin complex. Indeed, this is seen using a peptide containing the minimal region of Syn4 that binds F-actin (GFP-39–112), or through global F-actin depolymerization using the actin monomer binding agent LAT (10). Oddly, treatment with LAT failed to also elevate basal insulin secretion, suggesting that there is distinction between nonspecifically disrupting the entire F-actin cytoskeleton and disrupting select protein-protein interactions, as in the

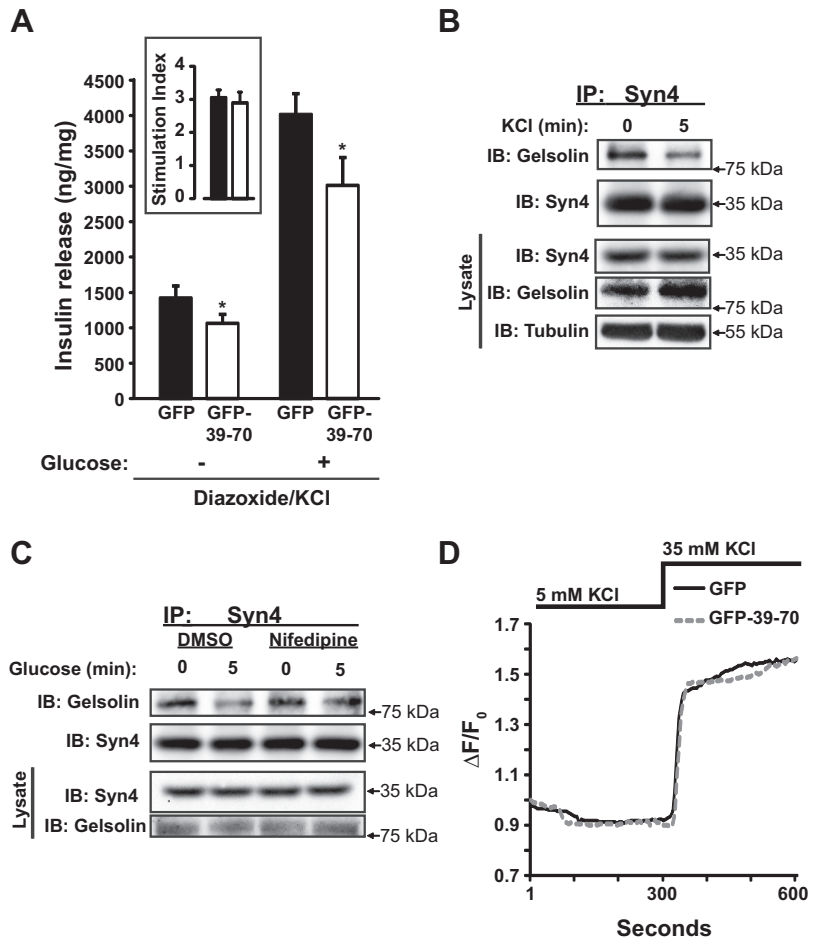

FIG. 8. Effects of GFP-39–70 upon the triggering pathway. A, Effects of GFP-39–70 were evaluated by the diazoxide paradigm. MIN6 cells transduced to express GFP or GFP-39–70 proteins were incubated with 250 μM diazoxide and 35 mM KCl, followed by addition of 20 mM glucose for 30 min and upon insulin secretion quantified. Insulin released was normalized for corresponding cellular protein content (nanograms of insulin/milligrams of protein). *Inset*, Stimulation index = insulin release under diazoxide + KCl + glucose treatment/insulin release under diazoxide + KCl treatment alone (*black bar*, GFP; *open bar*, GFP-39–70). Data represent the mean ± SE of at least three independent islet batches; *, $P < 0.05$ *vs.* GFP. B, MIN6 cells preincubated in MKRBB were stimulated 5 min with KCl (50 mM) and resultant cell lysates used for Syn4 immunoprecipitation (IP) as described in Fig. 1B. Data are representative of five independent experiments. C, MIN6 cells treated with vehicle [dimethylsulfoxide (DMSO)] or nifedipine for 1 h during preincubation in MKRBB were acutely stimulated with glucose (20 mM) for 5 min, in the continued presence of nifedipine/DMSO, and resultant cell lysates used in anti-Syn4 immunoprecipitation reactions. Protein abundances in starting input lysates (100 μg) were confirmed on a separate gel. Data are representative of three independent experiments. D, MIN6 cells on glass coverslips transduced to express GFP or GFP-39–70 proteins were preincubated in MKRBB supplemented with 2 mM glucose for 2 h followed by loading with fura 2-AM. Cells were subjected to perfusion for 300 sec under low KCl (5 mM) conditions and switched to buffer containing stimulatory KCl (35 mM) for an additional 300 sec to evaluate calcium influx. Each 340/380 ratio trace was normalized to the initial basal value (F_0) of the respective trace to yield $\Delta F/F_0$. IB, Immunoblotting.

case of using GFP-39–70 to disrupt Syn4-gelsolin complexes. The idea that basal insulin secretion is influenced by the cytoskeleton is supported by studies of EphA-Ephrin-A signaling, cell-cell contact, and focal adhesion kinase (23, 31, 32).

It is interesting that cells expressing GFP-39–70 and further subjected to acute glucose stimulation did not elicit an additive effect upon disruption of Syn4-gelsolin complexes, such that a contingent of complexes persisted. This phenomenon was also observed with peptide disruption of F-actin-Syn4 binding (10). One possibility is that the peptide is only capable of mimicking the action of secretagogue and only disrupts a subset of complexes; some may be refractory or inaccessible. Furthermore, it remains unknown as to whether Syn4 associates, transiently or otherwise, with gelsolin and/or F-actin during the dynamic process of SNARE complex assembly/disassembly; dissociation events may be so transient that it is not possible to detect all dissociated in sync. Although it also remains possible that the peptide is a relatively poor competitor, despite our lysate evidence showing it to be abundantly expressed, future studies of Syn4-gelsolin complex kinetics are required to address issues related to dissociation susceptibility.

In conclusion, we describe the first mechanistic evidence for gelsolin in regulating the exocytosis machinery, via its direct association with the t-SNARE protein Syn4. Through association with Syn4, gelsolin plays a critical role as a clamp on unsolicited Syn4 activation and aberrant insulin release in the absence of the appropriate secretagogue signal. Calcium may act as the key that unlocks the gelsolin clamp, because it is known to initiate gelsolin conformational changes. Once released from gelsolin, Syn4 activates and joins other SNARE proteins to facilitate granule docking and fusion. Importantly, elevated basal insulin release observed in islets with peptide-induced disruption of Syn4-gelsolin complexes models the constitutive insulin release observed in prediabetic and type 2 diabetic patients, before onset of β-cell apoptosis; this may provide new insight into the dysregulation of insulin exocytosis in diabetes. From a broader perspective, gelsolin and Syn4 are ubiquitously expressed proteins, such that their interaction may represent a more generalized clamping mechanism required for maintaining the "regulated" aspect of SNARE-mediated exocytosis.

Materials and Methods

Materials

Two rabbit polyclonal anti-Syn4 antibodies were obtained for use in coimmunoprecipitation (Chemicon, Temecula, CA) and for immunoblotting (in-house, described in Ref. 41). Rabbit anti-GFP and anti-glyceraldehyde-3-phosphate dehydrogenase antibodies were obtained from Abcam (Cambridge, MA). Monoclonal mouse anti-GFP, mouse anti-Cdc42, and mouse antigelsolin antibodies were purchased from CLONTECH/BD Biosciences (Mountain View, CA). Rabbit anti-actin antibody, Flag-M2 antibody, 4′,6-diamidino-2-phenylindole (DAPI), nifedipine, and diazoxide were purchased from Sigma (St. Louis, MO). LAT was obtained from Calbiochem (San Diego, CA). Rabbit anti-GST was obtained from Affinity Bioreagents (Golden, CO). Rabbit antiphospho-αPak1 (Thr423) was purchased from Santa Cruz Biotechnology, Inc. (Santa Cruz, CA). Rabbit IgG and rabbit anti-Pak1 were purchased from Cell Signaling (Danvers, MA). Fura 2-AM and rhodamine-phalloidin were purchased from Invitrogen (Carlsbad, CA). The MIN6 cells were a gift from John Hutton (University of Colorado Health Sciences Center, Denver, CO). Goat antimouse horseradish peroxidase secondary antibody was obtained from Thermo Fisher Scientific (Rockford, IL). Goat antirabbit horseradish peroxidase secondary antibody and TransFectin lipid reagent were acquired from Bio-Rad (Hercules, CA). enhanced chemiluminescence reagent and Supersignal Femto were purchased from GE Healthcare (Piscataway, NJ) and Pierce (Rockford, IL), respectively. The rat insulin RIA kits were obtained from Millipore (Billerica, MA).

Plasmids

The pGEX4T-1 plasmids containing rat Syn4 residues 1–273, 1–194, 1–112, and 1–70 and pEGFP-C2 plasmids containing Syn4 residues 1–273, 1–194, and 39–112 were previously described (10). A PCR-generated DNA insert comprising the 39–70 residue region of Syn4 was subcloned into the 5′ *Eco*RI and 3′ *Xho*I sites of the pEGFP-C2 vector (CLONTECH) to generate pEGFP-Syn4–39-70; GFP-Scr (scrambled helical peptide) was inserted similarly using annealed primer set sequences: 5′sense strand, attcatgaagttct tcgacaccaagaaggtggagctggagctgacccagatcgtgcagatggagcagatcgagc agctgagcaggaagcagaccagggccgtgtagg-3′. GFP-Scr helicity was predicted to be 87.5%, that closest in helicity to GFP-39–70 that also failed to match with any known mouse peptides in BLAST. The pGFP-39–70-Ad adenoviral expression plasmid was generated by subcloning the GFP-39–70 DNA into the 5′ *Bam*HI and 3′ *Not*I sites of the pAdCMVK vector (Viraquest, Inc., North Liberty, IA), after which adenoviral production was carried out by Viraquest, Inc. The pIRES-GFP-gelsolin-Flag plasmid was generated by subcloning DNA comprising only the cytoplasmic isoform (missing residues 1–50 of full-length protein) from the full-length mouse cDNA purchased from Open Biosystems (Huntsville, AL) into the 5′ *Nhe*I and 3′ *Xho*I sites of the pIRES-GFP-3XFlag vector; the modified vector was a gift of Raj Khanna (Indiana University School of Medicine). All constructs were verified by DNA sequencing.

Recombinant proteins and interaction assays

All GST fusion proteins were expressed in *Escherichia coli* and purified by glutathione-sepharose affinity chromatography as described previously (10). GST-Syn4 truncation GST proteins (20 μg) immobilized on sepharose beads were incubated with 20 μg of recombinant his-tagged human gelsolin protein (Cytoskeleton, Inc., Denver, CO) in a 0.25% Nonidet P-40 (NP-40) containing lysis buffer [25 mM HEPES (pH 7.4), 0.25% NP-40, 10% glycerol, 50 mM sodium fluoride, 10 mM sodium pyrophosphate, 137 mM NaCl, 1 mM sodium vanadate, 1 mM phenylmethylsulfonyl fluoride, 10 μg/ml aprotinin, 1 μg/ml pepstatin, and 5 μg/ml leupeptin] for 2 h at 4 C. After three washes with PBS, bound proteins were eluted from the sepharose beads and proteins resolved on 10% SDS-PAGE followed by transfer to polyvinylidene fluoride (PVDF) membrane for immunoblotting.

Cell culture, transient transfection, adenoviral transduction, and secretion assays

MIN6 β-cells were cultured in DMEM (25 mM glucose) supplemented with 15% fetal bovine serum, 100 U/ml penicillin, 100 μg/ml streptomycin, 292 μg/ml L-glutamine, and 50 μM β-mercaptoethanol as described previously (69). MIN6 β-cells at approximately 60–70% confluence were transfected using cesium chloride-purified plasmid DNA with TransFectin (Bio-Rad) to obtain approximately 30–50% transfection efficiency. Electroporation of MIN6 cells was carried out as previously described (71). After 48 h of incubation, cells were washed twice with and incubated for 2 h in freshly prepared modified Krebs-Ringer bicarbonate buffer (MKRBB) [5 mM KCl, 120 mM NaCl, 15 mM HEPES (pH 7.4), 24 mM $NaHCO_3$, 1 mM $MgCl_2$, 2 mM $CaCl_2$, and 1 mg/ml RIA-grade BSA]. Cells were stimulated with 20 mM glucose for the times indicated in the figures, after which the buffer was collected and centrifuged for 10 min at 4 C to pellet cell debris and insulin secreted into the buffer was quantitated using a rat insulin RIA kit (Millipore). Cells were harvested in 1% NP-40 lysis buffer (same as 0.25% NP-40 with exception of 1% NP-40), lysed for 10 min at 4 C, and were cleared of insoluble material by centrifugation for 10 min at 4 C for subsequent use in coimmunoprecipitation experiments. For adenoviral overexpression, MIN6 cells at 50–60% confluence were transduced at an multiplicity of infection of 100 for 2 h, washed twice with PBS, and incubated in complete media for 48 h. Cells were subsequently preincubated in MKRBB, subjected to stimulation, and harvested for generation of detergent cell lysates as described above.

Coimmunoprecipitation and immunoblotting

For each immunoprecipitation, 2–3 mg of cleared detergent lysate protein were combined with 1 μg of antibody per milligram of protein and the reaction rotated for 2 h at 4 C. Protein G Plus agarose beads (Santa Cruz Biotechnology, Inc.) were added and reactions rotated at 4 C for an additional 2 h. Beads were pelleted and washed three times with lysis buffer, and resulting immunoprecipitates were resolved on 10–12% SDS-PAGE and transfer to PVDF membranes for immunoblotting. Immunoreactive bands were visualized with enhanced chemiluminescence or Supersignal Femto reagents and imaged using a Chemi-Doc gel documentation system (Bio-Rad).

Calcium imaging

MIN6 cells transduced as described above were preincubated in MKRBB for 2 h, with fura 2-AM (5 μM) added to the cells for an additional 25 min as reported previously (72, 73). Cells were

washed with MKRBB to remove excess fura 2-AM and placed in fresh MKRBB containing low (2 mM) glucose and KCl (5 mM). Cells were imaged under constant perfusion (1 ml/min) for 300 sec, followed by stimulation with 35 mM KCl to elicit calcium influx for 300 sec. Fura 2-AM was excited at 340 and 380 nm and emission captured at 510 nm on a Zeiss Axio Observer Apochromat 100X/1.46 objective equipped with a Hamamastu Orca-ER digital camera and analyzed using AxioVision 4.7 software (Carl Zeiss, Oberkochen, Germany). Fura 2 has been shown to exhibit similar fluorescence from cells untransfected or transfected with GFP (74).

Immunofluorescence and confocal microscopy

MIN6 cells plated onto glass coverslips at 30% confluence were transiently transfected with 4 μg of plasmid DNA/35-mm well. After a 48-h incubation, cells were placed in MKRBB for 2 h, followed by stimulation with 20 mM glucose for 5 min, and then immediately fixed and permeabilized in 4% paraformaldehyde and 0.1% Triton X-100 for 10 min at 4 C. Fixed and permeabilized cells were blocked in 1% BSA plus 5% donkey serum for 1 h at room temperature, followed by incubation with 0.17 μM rhodamine-phalloidin for 1 h, per manufacturer instructions. MIN6 cells were then washed three times with PBS (pH 7.4). During the final wash, 4′,6-diamidino-2-phenylindole was added to stain nuclei. All cells were washed again with PBS and mounted (using Vectashield) for confocal fluorescence microscopy. GFP and rhodamine fluorescing cells were imaged using single-channel scanning with a $\times$60 objective under a $\times$2 zoom using an Olympus FV1000-MPE confocal microscope (Olympus, Center Valley, PA).

Mouse islet isolation, transduction, perifusion, and static culture

All studies involving mice followed the Guidelines for the Use and Care of Laboratory Animals at Indiana University School of Medicine. Wild-type male C57BL/6J mice were killed for pancreatic islet isolation as previously described (7). All viruses were obtained from Viraquest, Inc. Freshly isolated islets were immediately transduced with 10^7 plaque-forming unit/islet with either GFP-Ad or GFP-39–70-Ad CsCl-purified particles for 1 h at 37 C in RPMI 1640 medium, washed twice with PBS, and incubated 48 h at 37 C/5% CO_2. GFP fluorescence was visualized in greater than 60–70% of islet cells with even penetration to the islet core. GFP positive islets were handpicked into batches of 10/tube for static secretion studies or 50 islets/column for perifusion. Perifusion studies were carried out as previously described (75). Islet batches were incubated 2 h in Kreb's ringer bicarbonate hepes buffer [10 mM HEPES (pH 7.4), 134 mM NaCl, 5 mM $NaHCO_3$, 4.8 mM KCl, 1 mM $CaCl_2$, 1.2 mM $MgSO_4$, and 1.2 mM KH_2PO_4 containing 0.5 mg/ml BSA] supplemented with 2.8 mM glucose, followed by 1 h incubation in either 2.8 or 16.7 mM glucose. Insulin secreted into the buffer and insulin content in the corresponding islet lysates was quantified by Rat Insulin RIA (Millipore).

Statistical analysis

All quantitated data are expressed as mean $\pm$ SE. Data were evaluated using Student's t test and considered significant if $P < 0.05$.

Acknowledgments

We thank Dr. Eunjin Oh for her assistance and technical expertise and Dr. Jenna Jewell, Dr. Vinnie Tagliabracci, and Latha Ramalingam for many helpful discussions. MIN6 cells and the modified pIRES-GFP-3X flag vector were kindly provided by Dr. John Hutton (Denver, CO) and Dr. Raj Khanna (Indianapolis, IN), respectively.

Address all correspondence and requests for reprints to: Debbie C. Thurmond, Ph.D., 635 Barnhill Drive, MS2031, Indianapolis, Indiana 46202. E-mail: dthurmon@iupui.edu.

This work was supported by National Institutes of Health Grants DK076614 and DK067912 (to D.C.T.), DK087811 (to D.A.W.), and CTSI-KL2 RR025760 (to Z.W.); the American Heart Association predoctoral fellowship 10PRE3040010 (to M.A.K.); and the NIH predoctoral fellowship T32DK64466 (to M.A.K.).

Disclosure Summary: The authors have nothing to disclose.

References

1. **Grodsky GM** 2000 Kinetics of insulin secretion: underlying metabolic events. In: LeRoith D, Taylor S, Olefsky J, eds. Diabetes mellitus: a fundamental and clinical text. Philadelphia: Lippincott Williams & Wilkins
2. **Rorsman P, Eliasson L, Renström E, Gromada J, Barg S, Göpel S** 2000 The cell physiology of biphasic insulin secretion. News Physiol Sci 15:72–77
3. **Regazzi R, Wollheim CB, Lang J, Theler JM, Rossetto O, Montecucco C, Sadoul K, Weller U, Palmer M, Thorens B** 1995 VAMP-2 and cellubrevin are expressed in pancreatic β-cells and are essential for Ca(2+)-but not for GTP γ S-induced insulin secretion. EMBO J 14:2723–2730
4. **Sadoul K, Lang J, Montecucco C, Weller U, Regazzi R, Catsicas S, Wollheim CB, Halban PA** 1995 SNAP-25 is expressed in islets of Langerhans and is involved in insulin release. J Cell Biol 128:1019–1028
5. **Kiraly-Borri CE, Morgan A, Burgoyne RD, Weller U, Wollheim CB, Lang J** 1996 Soluble N-ethylmaleimide-sensitive-factor attachment protein and N-ethylmaleimide-insensitive factors are required for Ca2+-stimulated exocytosis of insulin. Biochem J 314:199–203
6. **Jacobsson G, Bean AJ, Scheller RH, Juntti-Berggren L, Deeney JT, Berggren PO, Meister B** 1994 Identification of synaptic proteins and their isoform mRNAs in compartments of pancreatic endocrine cells. Proc Natl Acad Sci USA 91:12487–12491
7. **Spurlin BA, Thurmond DC** 2006 Syntaxin 4 facilitates biphasic glucose-stimulated insulin secretion from pancreatic β-cells. Mol Endocrinol 20:183–193
8. **Ohara-Imaizumi M, Fujiwara T, Nakamichi Y, Okamura T, Akimoto Y, Kawai J, Matsushima S, Kawakami H, Watanabe T, Akagawa K, Nagamatsu S** 2007 Imaging analysis reveals mechanistic differences between first- and second-phase insulin exocytosis. J Cell Biol 177:695–705
9. **Thurmond DC, Gonelle-Gispert C, Furukawa M, Halban PA, Pessin JE** 2003 Glucose-stimulated insulin secretion is coupled to the interaction of actin with the t-SNARE (target membrane soluble N-ethylmaleimide-sensitive factor attachment protein receptor protein) complex. Mol Endocrinol 17:732–742
10. **Jewell JL, Luo W, Oh E, Wang Z, Thurmond DC** 2008 Filamentous actin regulates insulin exocytosis through direct interaction with syntaxin 4. J Biol Chem 283:10716–10726
11. **Wheeler MB, Sheu L, Ghai M, Bouquillon A, Grondin G, Weller U,**

Beaudoin AR, Bennett MK, Trimble WS, Gaisano HY 1996 Characterization of SNARE protein expression in β cell lines and pancreatic islets. Endocrinology 137:1340–1348
12. **Jahn R, Scheller RH** 2006 SNAREs— engines for membrane fusion. Nat Rev Mol Cell Biol 7:631–643
13. **Chen YA, Scheller RH** 2001 SNARE-mediated membrane fusion. Nat Rev Mol Cell Biol 2:98–106
14. **Leahy JL, Fineman MS** 1998 Impaired phasic insulin and amylin secretion in diabetic rats. Am J Physiol 275:E457–E462
15. **Varadi A, Tsuboi T, Rutter GA** 2005 Myosin Va transports dense core secretory vesicles in pancreatic MIN6 β-cells. Mol Biol Cell 16:2670–2680
16. **Nevins AK, Thurmond DC** 2003 Glucose regulates the cortical actin network through modulation of Cdc42 cycling to stimulate insulin secretion. Am J Physiol Cell Physiol 285:C698–C710
17. **Orci L, Gabbay KH, Malaisse WJ** 1972 Pancreatic β-cell web: its possible role in insulin secretion. Science 175:1128–1130
18. **Aunis D, Bader MF** 1988 The cytoskeleton as a barrier to exocytosis in secretory cells. J Exp Biol 139:253–266
19. **Mourad NI, Nenquin M, Henquin JC** 2010 Metabolic amplifying pathway increases both phases of insulin secretion independently of β-cell actin microfilaments. Am J Physiol Cell Physiol 299:C389–C398
20. **Schubert S, Knoch KP, Ouwendijk J, Mohammed S, Bodrov Y, Jäger M, Altkrüger A, Wegbrod C, Adams ME, Kim Y, Froehner SC, Jensen ON, Kalaidzidis Y, Solimena M** 2010 β2-Syntrophin is a Cdk5 substrate that restrains the motility of insulin secretory granules. PLoS One 5:e12929
21. **Snabes MC, Boyd 3rd AE** 1982 Increased filamentous actin in islets of Langerhans from fasted hamsters. Biochem Biophys Res Commun 104:207–211
22. **Swanston-Flatt SK, Carlsson L, Gylfe E** 1980 Actin filament formation in pancreatic β-cells during glucose stimulation of insulin secretion. FEBS Lett 117:299–302
23. **Konstantinova I, Nikolova G, Ohara-Imaizumi M, Meda P, Kucera T, Zarbalis K, Wurst W, Nagamatsu S, Lammert E** 2007 EphA-ephrin-A-mediated β cell communication regulates insulin secretion from pancreatic islets. Cell 129:359–370
24. **Howell SL, Tyhurst M** 1980 The role of actin in the secretory cycle. Horm Metab Res Suppl 10(Suppl):168–171
25. **Lacy PE, Walker MM, Fink CJ** 1972 Perifusion of isolated rat islets in vitro. Participation of the microtubular system in the biphasic release of insulin. Diabetes 21:987–998
26. **Langford GM** 2002 Myosin-V, a versatile motor for short-range vesicle transport. Traffic 3:859–865
27. **Eitzen G** 2003 Actin remodeling to facilitate membrane fusion. Biochim Biophys Acta 1641:175–181
28. **Woronowicz K, Dilks JR, Rozenvayn N, Dowal L, Blair PS, Peters CG, Woronowicz L, Flaumenhaft R** 2010 The platelet actin cytoskeleton associates with SNAREs and participates in α-granule secretion. Biochemistry 49:4533–4542
29. **Lang T, Wacker I, Wunderlich I, Rohrbach A, Giese G, Soldati T, Almers W** 2000 Role of actin cortex in the subplasmalemmal transport of secretory granules in PC-12 cells. Biophys J 78:2863–2877
30. **Torregrosa-Hetland CJ, Villanueva J, Giner D, Lopez-Font I, Nadal A, Quesada I, Viniegra S, Expósito-Romero G, Gil A, Gonzalez-Velez V, Segura J, Gutiérrez LM** 2011 The F-actin cortical network is a major factor influencing the organization of the secretory machinery in chromaffin cells. J Cell Sci 124:727–734
31. **Rondas D, Tomas A, Halban PA** 2011 Focal adhesion remodeling is crucial for glucose-stimulated insulin secretion and involves activation of focal adhesion kinase and paxillin. Diabetes 60:1146–1157
32. **Jaques F, Jousset H, Tomas A, Prost AL, Wollheim CB, Irminger JC, Demaurex N, Halban PA** 2008 Dual effect of cell-cell contact disruption on cytosolic calcium and insulin secretion. Endocrinology 149:2494–2505
33. **Band AM, Ali H, Vartiainen MK, Welti S, Lappalainen P, Olkkonen VM, Kuismanen E** 2002 Endogenous plasma membrane t-SNARE syntaxin 4 is present in rab11 positive endosomal membranes and associates with cortical actin cytoskeleton. FEBS Lett 531:513–519
34. **Wang Z, Thurmond DC** 2010 Differential phosphorylation of RhoGDI mediates the distinct cycling of Cdc42 and Rac1 to regulate second-phase insulin secretion. J Biol Chem 285:6186–6197
35. **Wang Z, Oh E, Thurmond DC** 2007 Glucose-stimulated Cdc42 signaling is essential for the second phase of insulin secretion. J Biol Chem 282:9536–9546
36. **Tomas A, Yermen B, Min L, Pessin JE, Halban PA** 2006 Regulation of pancreatic β-cell insulin secretion by actin cytoskeleton remodelling: role of gelsolin and cooperation with the MAPK signalling pathway. J Cell Sci 119:2156–2167
37. **Nelson TY, Boyd 3rd AE** 1985 Gelsolin, a Ca2+-dependent actin-binding protein in a hamster insulin-secreting cell line. J Clin Invest 75:1015–1022
38. **Jewell JL, Oh E, Bennett SM, Meroueh SO, Thurmond DC** 2008 The tyrosine phosphorylation of Munc18c induces a switch in binding specificity from syntaxin 4 to Doc2β. J Biol Chem 283:21734–21746
39. **Yermen B, Tomas A, Halban PA** 2007 Pro-survival role of gelsolin in mouse β-cells. Diabetes 56:80–87
40. **Witke W, Sharpe AH, Hartwig JH, Azuma T, Stossel TP, Kwiatkowski DJ** 1995 Hemostatic, inflammatory, and fibroblast responses are blunted in mice lacking gelsolin. Cell 81:41–51
41. **Wiseman DA, Kalwat MA, Thurmond DC** 2011 Stimulus-induced S-nitrosylation of syntaxin 4 impacts insulin granule exocytosis. J Biol Chem 286:16344–16354
42. **Nevins AK, Thurmond DC** 2006 Caveolin-1 functions as a novel Cdc42 guanine nucleotide dissociation inhibitor in pancreatic β-cells. J Biol Chem 281:18961–18972
43. **Ishihara H, Asano T, Tsukuda K, Katagiri H, Inukai K, Anai M, Kikuchi M, Yazaki Y, Miyazaki JI, Oka Y** 1993 Pancreatic β cell line MIN6 exhibits characteristics of glucose metabolism and glucose-stimulated insulin secretion similar to those of normal islets. Diabetologia 36:1139–1145
44. **Henquin JC** 2000 Triggering and amplifying pathways of regulation of insulin secretion by glucose. Diabetes 49:1751–1760
45. **Bratanova-Tochkova TK, Cheng H, Daniel S, Gunawardana S, Liu YJ, Mulvaney-Musa J, Schermerhorn T, Straub SG, Yajima H, Sharp GW** 2002 Triggering and augmentation mechanisms, granule pools, and biphasic insulin secretion. Diabetes 51:S83–90
46. **Straub SG, Sharp GW** 2002 Glucose-stimulated signaling pathways in biphasic insulin secretion. Diabetes Metab Res Rev 18:451–463
47. **Ohara-Imaizumi M, Nakamichi Y, Tanaka T, Ishida H, Nagamatsu S** 2002 Imaging exocytosis of single insulin secretory granules with evanescent wave microscopy: distinct behavior of granule motion in biphasic insulin release. J Biol Chem 277:3805–3808
48. **Gembal M, Gilon P, Henquin JC** 1992 Evidence that glucose can control insulin release independently from its action on ATP-sensitive K+ channels in mouse B cells. J Clin Invest 89:1288–1295
49. **Henquin JC, Ishiyama N, Nenquin M, Ravier MA, Jonas JC** 2002 Signals and pools underlying biphasic insulin secretion. Diabetes 51:S60–S67
50. **Spinardi L, Witke W** 2007 Gelsolin and diseases. Subcell Biochem 45:55–69
51. **Rutter GA, Tsuboi T, Ravier MA** 2006 Ca2+ microdomains and the control of insulin secretion. Cell Calcium 40:539–551
52. **Nightingale TD, White IJ, Doyle EL, Turmaine M, Harrison-Lavoie KJ, Webb KF, Cramer LP, Cutler DF** 2011 Actomyosin II contractility expels von Willebrand factor from Weibel-Palade bodies during exocytosis. J Cell Biol 194:613–629
53. **Yin HL, Stossel TP** 1979 Control of cytoplasmic actin gel-sol transformation by gelsolin, a calcium-dependent regulatory protein. Nature 281:583–586

54. **Choe H, Burtnick LD, Mejillano M, Yin HL, Robinson RC, Choe S** 2002 The calcium activation of gelsolin: insights from the 3A structure of the G4–G6/actin complex. J Mol Biol 324:691–702
55. **Burtnick LD, Koepf EK, Grimes J, Jones EY, Stuart DI, McLaughlin PJ, Robinson RC** 1997 The crystal structure of plasma gelsolin: implications for actin severing, capping, and nucleation. Cell 90: 661–670
56. **Casimir M, Dai XQ, Hajmrle C, Kolic J, Guo D, Oudit G, MacDonald PE** 2011 Gelsolin knockout impairs insulin secretion independently of actin polymerization. Diabetes 60:A351
57. **Azuma T, Witke W, Stossel TP, Hartwig JH, Kwiatkowski DJ** 1998 Gelsolin is a downstream effector of rac for fibroblast motility. EMBO J 17:1362–1370
58. **Furukawa K, Fu W, Li Y, Witke W, Kwiatkowski DJ, Mattson MP** 1997 The actin-severing protein gelsolin modulates calcium channel and NMDA receptor activities and vulnerability to excitotoxicity in hippocampal neurons. J Neurosci 17:8178–8186
59. **Janmey PA, Stossel TP** 1987 Modulation of gelsolin function by phosphatidylinositol 4,5-bisphosphate. Nature 325:362–364
60. **Tomas A, Yermen B, Regazzi R, Pessin JE, Halban PA** 2010 Regulation of insulin secretion by phosphatidylinositol-4,5-bisphosphate. Traffic 11:123–137
61. **El Sayegh TY, Arora PD, Ling K, Laschinger C, Janmey PA, Anderson RA, McCulloch CA** 2007 Phosphatidylinositol-4,5 bisphosphate produced by PIP5KIγ regulates gelsolin, actin assembly, and adhesion strength of N-cadherin junctions. Mol Biol Cell 18:3026–3038
62. **Lueck A, Brown D, Kwiatkowski DJ** 1998 The actin-binding proteins adseverin and gelsolin are both highly expressed but differentially localized in kidney and intestine. J Cell Sci 111(Pt 24):3633–3643
63. **Bruun TZ, Høy M, Gromada J** 2000 Scinderin-derived actin-binding peptides inhibit Ca(2+)- and GTPγS-dependent exocytosis in mouse pancreatic β-cells. Eur J Pharmacol 403:221–224
64. **Sørensen JB, Matti U, Wei SH, Nehring RB, Voets T, Ashery U, Binz T, Neher E, Rettig J** 2002 The SNARE protein SNAP-25 is linked to fast calcium triggering of exocytosis. Proc Natl Acad Sci USA 99:1627–1632
65. **Wiser O, Trus M, Hernández A, Renström E, Barg S, Rorsman P, Atlas D** 1999 The voltage sensitive Lc-type Ca2+ channel is functionally coupled to the exocytotic machinery. Proc Natl Acad Sci USA 96:248–253
66. **Yang SN, Larsson O, Bränström R, Bertorello AM, Leibiger B, Leibiger IB, Moede T, Köhler M, Meister B, Berggren PO** 1999 Syntaxin 1 interacts with the L(D) subtype of voltage-gated Ca(2+) channels in pancreatic β cells. Proc Natl Acad Sci USA 96:10164–10169
67. **Gustavsson N, Lao Y, Maximov A, Chuang JC, Kostromina E, Repa JJ, Li C, Radda GK, Südhof TC, Han W** 2008 Impaired insulin secretion and glucose intolerance in synaptotagmin-7 null mutant mice. Proc Natl Acad Sci USA 105:3992–3997
68. **Gauthier BR, Duhamel DL, Iezzi M, Theander S, Saltel F, Fukuda M, Wehrle-Haller B, Wollheim CB** 2008 Synaptotagmin VII splice variants α, β, and δ are expressed in pancreatic β-cells and regulate insulin exocytosis. FASEB J 22:194–206
69. **Ke B, Oh E, Thurmond DC** 2007 Doc2β is a novel Munc18c-interacting partner and positive effector of syntaxin 4-mediated exocytosis. J Biol Chem 282:21786–21797
70. **Verhage M, de Vries KJ, Røshol H, Burbach JP, Gispen WH, Südhof TC** 1997 DOC2 proteins in rat brain: complementary distribution and proposed function as vesicular adapter proteins in early stages of secretion. Neuron 18:453–461
71. **Oh E, Thurmond DC** 2006 The stimulus-induced tyrosine phosphorylation of Munc18c facilitates vesicle exocytosis. J Biol Chem 281:17624–17634
72. **Lopez JP, Turner JR, Philipson LH** 2010 Glucose-induced ERM protein activation and translocation regulates insulin secretion. Am J Physiol Endocrinol Metab 299:E772–E785
73. **Yaekura K, Julyan R, Wicksteed BL, Hays LB, Alarcon C, Sommers S, Poitout V, Baskin DG, Wang Y, Philipson LH, Rhodes CJ** 2003 Insulin secretory deficiency and glucose intolerance in Rab3A null mice. J Biol Chem 278:9715–9721
74. **Billing-Marczak K, Przybyszewska M, Kuźnicki J** 1999 Measurements of [Ca2+] using fura-2 in glioma C6 cells expressing calretinin with GFP as a marker of transfection: no Ca2+-buffering provided by calretinin. Biochim Biophys Acta 1449:169–177
75. **Oh E, Thurmond DC** 2009 Munc18c depletion selectively impairs the sustained phase of insulin release. Diabetes 58:1165–1174